Solar Energy Materials & Solar Cells 93 (2009) 1587–1591

Contents lists available at ScienceDirect

Solar Energy Materials & Solar Cells

journal homepage: www.elsevier.com/locate/solmat

Hybrid inverted bulk heterojunction solar cells with nanoimprinted TiO_2 nanopores

Woon-Hyuk Baek [a], Il Seo [a], Tae-Sik Yoon [a], Hyun Ho Lee [b], Chong Man Yun [a], Yong-Sang Kim [a,c,*]

[a] Department of Nano Science & Engineering, Myongji University, Gyeonggi 449-728, Republic of Korea
[b] Department of Chemical Engineering, Myongji University, Gyeonggi 449-728, Republic of Korea
[c] Department of Electrical Engineering, Myongji University, Gyeonggi 449-728, Republic of Korea

ARTICLE INFO

Article history:
Received 20 November 2008
Received in revised form
7 April 2009
Accepted 11 April 2009
Available online 15 May 2009

Keywords:
Nanoporous TiO_2
Organic solar cells
Hybrid solar cells
Interface area
Inverted structure

ABSTRACT

Photovoltaic devices with highly ordered nanoporous titanium dioxide (titania; TiO_2) were fabricated to improve the photovoltaic performances by increasing TiO_2 interface area. The nanoimprinting lithography technique with polymethyl methacrylate (PMMA) mold was used to form titania nanopores. The solar cell with poly(3-hexylthiophene) (P3HT):[6,6]-phenyl C_{61} butyric acid methyl ester (PCBM) active layer on nanoporous titania showed higher power conversion efficiency (PCE) of 1.49% than on flat titania of 1.18%. The improved efficiency using nanoporous titania is interpreted with the enhanced-charge separation and collection by increasing the interface area between TiO_2 and active layer.

1. Introduction

Photovoltaic cells based on conjugated polymer and fullerene bulk heterojunction composites have the potential for renewable energy resources due to their lightness, low cost and simple fabrication processing in large area [1–8]. Recent studies have reported remarkably improved performances of the bulk heterojunction solar cells up to 5% in single-device structure [8,9]. However, there have been reported problems with oxides and organic materials in terms of stability. For example, especially the poly(phenylene vinylene) (PPV) is not stable in the presence of oxides which photo-oxidize the organic materials [10–14]. For the case of poly(3-hexylthiophene) (P3HT) with the oxides, however, the photo-oxidation is not so severe that it can be made air-stable hybrid devices [15,16]. As a consequence, from material point of view, poly(3,4-ethylenedioxythiophene):poly(styrene sulfonate) (PEDOT:PSS) as anodic buffer layer and P3HT with [6,6]-phenyl C_{61} butyric acid methyl ester (PCBM) blend as active layer represent for the state-of-the-art system.

In the conventional bulk heterojunction structure, however, acidic anodic buffer layer PEDOT:PSS has been proved to be deteriorative to the active layer, particularly under humid condition in the case of aluminum electrodes [17–19]. At the same time, it is known to be unstable in air, under illumination or on common electrodes such as indium tin oxide (ITO) from water adsorption by the PEDOT:PSS layer and presence of oxygen throughout the active layers [20–25]. In order to relieve these problems, many studies have been focused on searching alternative materials to the PEDOT:PSS layer in the inverted bulk heterojunction solar cell structure. These include highly transparent metal oxide [i.e. vanadium oxide (V_2O_5) and molybdenum oxide (MoO_3) [26], gold nanoparticle layer [27], TiO_2 nanotube arrays [28] and solution-processed titanium oxide (TiO_x) [29], zinc oxide (ZnO) [30] and cesium carbonate (Cs_2CO_3) [31]. However, the power conversion efficiency (PCE) of inverted solar cell structure is still behind that of conventional structure. Compared to the conventional structure with organic–organic interface (P3HT:PCBM–PEDOT), the inverted structure with organic–inorganic (P3HT:PCBM–TiO_2) interface leads to worse properties of exciton generation and separation. On the other hand, the inverted structure with TiO_2 is expected to achieve stable electron diffusion, electron selective transportation with high hole blocking barrier of TiO_2 and additional charge generation of P3HT–TiO_2 interface.

In this study, we improve the photovoltaic performances of solar cells fabricated with nanoimprinted nanoporous TiO_2 by increasing the interface area in the inverted solar cell structure ITO/TiO_2/P3HT:PCBM/Au. It is believed that both P3HT–PCBM and P3HT–TiO_2 interfaces result in more efficient charge separations

* Corresponding author at: Department of Nano Science & Engineering, Myongji University, Gyeonggi 449-728, Republic of Korea. Tel.: +81 31 338 6327; fax: +81 31 321 0271.
E-mail address: kys@mju.ac.kr (Y.-S. Kim).

0927-0248/$ - see front matter © 2009 Elsevier B.V. All rights reserved.
doi:10.1016/j.solmat.2009.04.014

and collections with the nanoporous titania interfacing the active layer than with flat titania.

2. Experimental

P3HT (Rieke Metals, Inc.) and PCBM (Sigma-Aldrich) were used as active layers without any further purification. The P3HT and PCBM (1:1 weight ratio) were dissolved in chlorobenzene solvent with 3 wt% solution and stirred at 60 °C for 1 h. The titania sol–gel solution was prepared by mixing titanium (IV) ethoxide, HCl and isopropyl alcohol. We previously reported the fabrication technique for highly ordered TiO_2 nanopores using anodic aluminum oxide (AAO) which was obtained by two-step anodizing method [32]. The AAO has about 80 nm of diameter and 100 nm of depth. Polymethyl methacrylate (PMMA; Aldrich) with a molecular mass of 350 kg/mol was dissolved in chlorobenzene. Nanopoled PMMA was created by pouring the solution on the AAO and by allowing the solution to percolate within the nanopores with heat treatment at 150 °C for 3 h. The PMMA nanopoles were then separated from the template by a wet etching technique in 1.4% of $FeCl_3$/5 M HCl solution. The Al and alumina residues were completely removed by 10% of NaOH cleaning solution. ITO-coated (15 Ω/□) glass substrate was cleaned in ultrasonic bath with DI water, acetone and isopropyl alcohol for 15 min. Nano-patterned PMMA mold was embossed after spin coating TiO_2 solution at 2000 rpm on to ITO substrate. The initial pattern of AAO is replicated to final titania structure by nanoimprinting with PMMA mold. Then TiO_2 layer was sintered at 500 °C for 1 h in ambient condition to obtain TiO_2 anatase phase. The thickness of flat titania was 100 nm measured by the surface profiler (alpha-step 500). A 200-nm-thick photoactive layer (P3HT:PCBM) was deposited on TiO_2 nanopores or PEDOT layer by spin coating. Au (100 nm) anode was thermally evaporated through shadow mask defining active area of 0.1 cm^2. Thermal annealing was conducted at 150 °C for 10 min in oven under N_2 ambient. The entire fabrication process was conducted in air environment except for thermal annealing of active layer. For a comparison with conventional device performance, solar cells using PEDOT:PSS (Baytron P VP AI 4083; H.C. Stark) and Al were fabricated in the structure of ITO/PEDOT/P3HT:PCBM/Al. The annealing condition and the active layer thickness of conventional devices were same with inverted devices. The current density versus voltage characteristics were measured with Keithley 236 source measurement unit and solar simulator (YSS-E40, Yamashita denso) under AM 1.5 G (100 mW/cm^2) irradiation intensity. The total incident light intensity was calibrated with pyranometer (Eko MS-802) and standard reference silicon solar cell. The Brunauer–Emmett–Teller (BET) specific surface areas of the flat and nanoporous titania were measured by analyzing the N_2 adsorption–desorption isotherms at 77 K (Micromeritics, ASAP 2020). UV/visible spectrophotometer (Shimadzu UV-1601) was used to study absorption spectra of the P3HT:PCBM films on TiO_2 layer. The surface of nanoporous titania was characterized using field-emission scanning electron microscope (FE-SEM; LEO SUPRA 55, Carl Zeiss) and atomic force microscope (AFM; XE-100, Park Systems) in non-contact mode.

3. Results and discussion

Fig. 1 shows schematic diagram of the hybrid bulk heterojunction solar cell and its energy band structure. Since the conduction band of TiO_2 is similar to that of PCBM, electrons can transport to ITO electrode through TiO_2 with ease. Moreover, the valance band of TiO_2 is efficient to prevent back electron or hole transfer with its high-energy barrier.

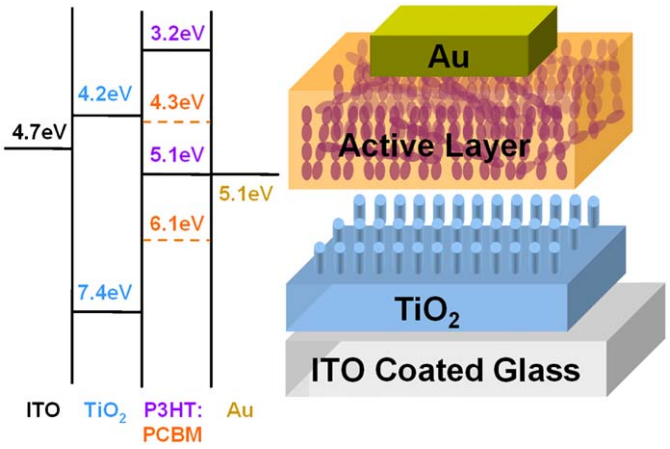

Fig. 1. Schematic diagram of the hybrid inverted bulk heterojunction solar cell and its energy band structure.

Fig. 2 shows FE-SEM and AFM images of nanoporous TiO_2. It shows that nanoporous titania was successfully fabricated using nanoimprinting lithography with PMMA nanopoles as a stamp. The initial film thickness of flat TiO_2 was 100 nm. The rms roughness extracted from AFM images of flat and nanoporous TiO_2 were ~1 and ~10 nm, respectively. The surface area is not always the function of roughness. BET analysis was conducted for both TiO_2 films. As the samples used for BET analysis were thin-film-coated ITO glass substrate, both thickness and weight of film significantly affect the surface area. Thereby, it is difficult to obtain exact number of surface area. We compared the results by preparing the samples to have same size and thickness. When we assume that the TiO_2 nanopores are perfect cylinder structures, the calculated increase of nanoporous TiO_2 surface area was about 60% than flat TiO_2. However, the measured surface area of nanoporous TiO_2 was increased about 40% than flat TiO_2. The mismatch was due to the defects resulted from various process steps to fabricate the nanoporous TiO_2. The increased rms roughness and surface area using nanoporous TiO_2 were expected to provide large interface between TiO_2 and active layer that would benefit for exciton generation and separation. The final titania nanopores have lager diameter (100 nm) and lower depth (30–40 nm) than AAO (80 nm of diameter and 100 nm of depth). The larger diameter of pores is thought to result from the lateral volume shrinkage of pore wall during sintering titania deposited from sol–gel solution. Also imprinting titania with PMMA mold compresses titania, thereby leaving shallower depth of pores. The pores with a size smaller than 20 nm would enhance the charge separation most effectively because a typical range of exciton diffusion length in polymers is 4–20 nm [33]. On the other hand, it is difficult to make polymer materials to self-organize and form close-chain packing structure inside such a small pore [34]. A relatively large size of nanopores in our structure is thought to enhance phase separation and allow the chain packing in active layer.

We previously observed that both the flat and nanoporous TiO_2 formed anatase phase with (1 0 1) preferred orientation on ITO substrate measured by X-ray diffraction (XRD) analysis [32]. The conduction band edge of TiO_2 anatase phase is about 0.2 eV higher than that of rutile TiO_2. Also, anatase phase facilitates electron transfer more than rutile and the higher energy barrier of anatase phase suppresses hole transfer or back electron transfer more effectively [35].

UV/visible absorption spectra in Fig. 3 shows that absorption of active layer coated on nanoporous TiO_2 was almost similar but slightly higher than that on flat TiO_2. Vibronic features of P3HT

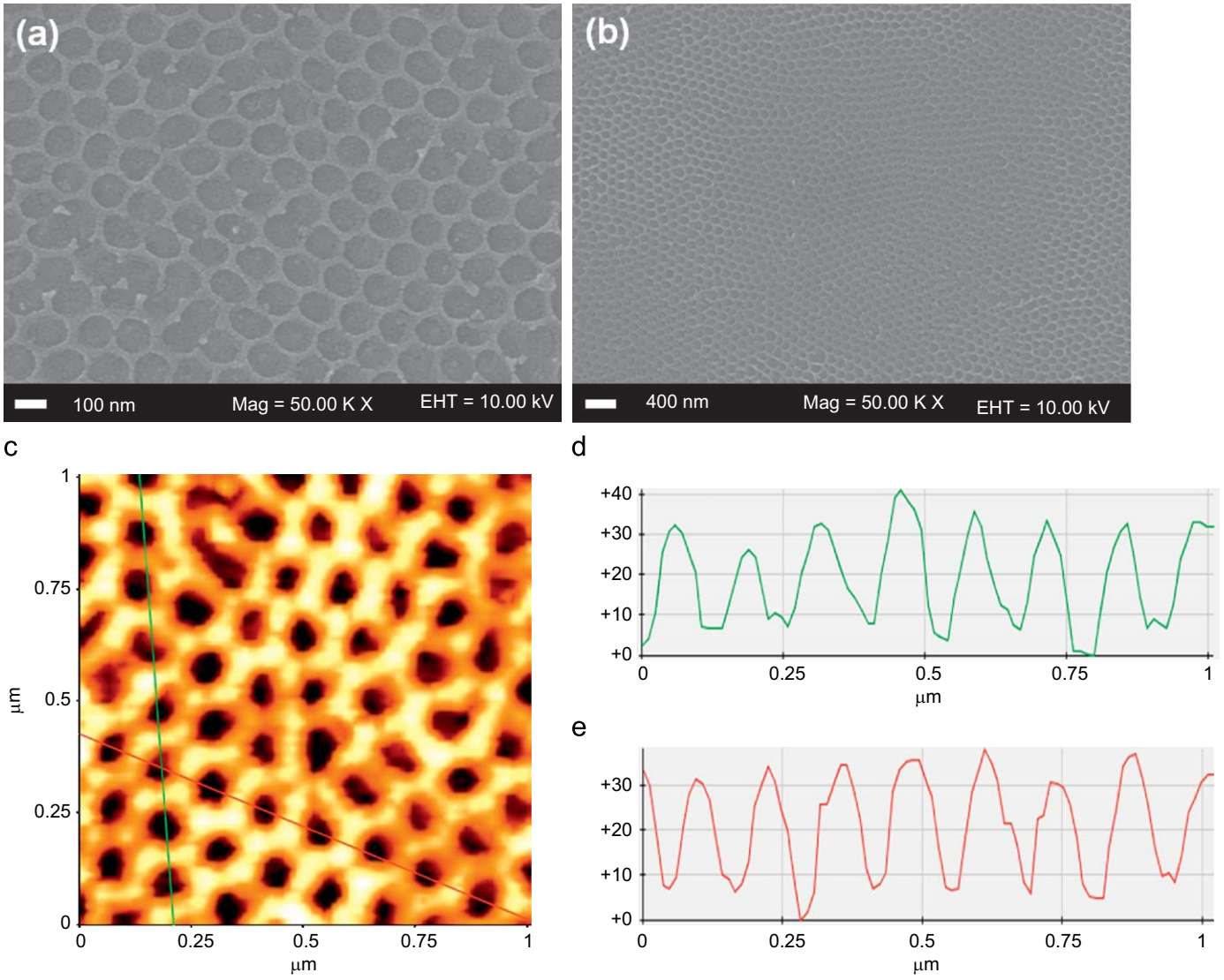

Fig. 2. FE-SEM (a, b) and AFM (c, d and e) images of nanoporous TiO_2; (a) top view, (b) large scale, (c) topography image and (d and e) line scan profile.

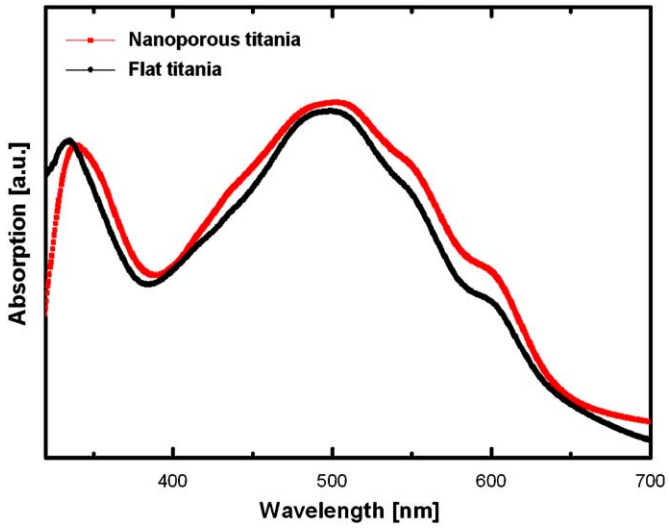

Fig. 3. UV/visible absorption spectra of active layer coated on flat and nanoporous TiO_2.

absorption from 450 to 650 nm wavelengths were also observed. In conjugated polymers, those features indicate high degree of polymer ordering implying long chain length and high crystallinity [36,37]. Therefore, the UV/visible results evidently indicate that a highly ordered active layer, even in the nanopores, was formed.

Current density–voltage (J–V) characteristic in Fig. 4 shows that short-circuit current (J_{sc}) and PCE were remarkably improved from 6.8 to 7.7 mA/cm^2 and 1.19% to 1.49%, respectively, by using nanoporous titania, while open circuit voltage (V_{oc}) and fill factor (FF) were slightly increased. Moreover, the device series resistance (R_s) decreases from 13.5 to 10.6 Ω cm^2 by using nanoporous titania. Series resistances were derived from slope of the J–V characteristics under illumination close to 1 V. It is thought that the improved efficiency using nanoporous titania results from the efficient charge separation by increasing interface area of P3HT–TiO_2 and reduced effective series resistance for electrons transporting to TiO_2 layer.

To be compared with the conventional device performance, solar cells using PEDOT:PSS buffer layer and Al electrode were fabricated in the structure of ITO/PEDOT/P3HT:PCBM/Al. Although

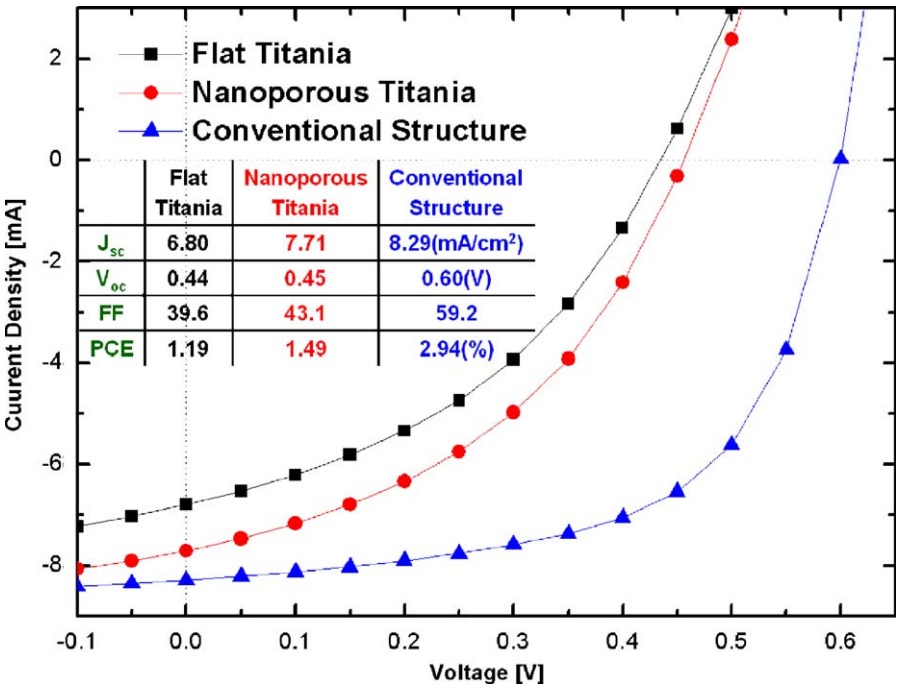

Fig. 4. Current density–voltage characteristics of conventional structure with PEDOT and hybrid inverted bulk heterojunction solar cells with flat and nanoporous TiO_2 at an irradiation intensity of 100 mW/cm^2.

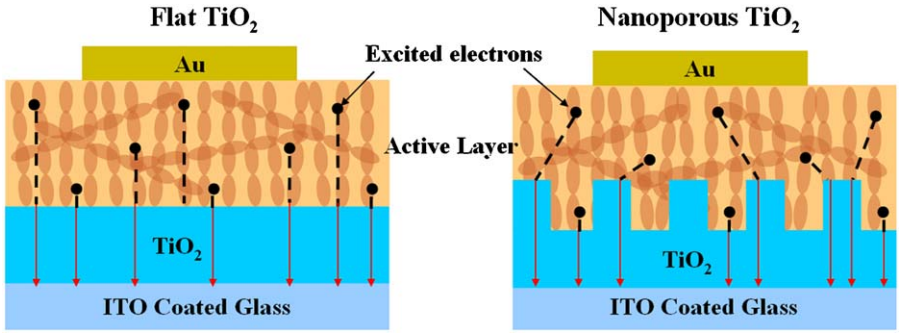

Fig. 5. Schematic different electron transportation concept of flat and nanoporous TiO_2.

J_{sc} of inverted architecture shows comparable results with that of conventional structure, V_{oc} and FF of the inverted structure were considerably poor. Like the reported literatures concerning about inverted structure with titanium oxide [28,29,38], PEDOT was used as interlayer between active layer and top electrode, thereby it shows comparable results with conventional structure. Nevertheless, this architecture still has degradation problem of PEDOT in the humid or illuminated condition, though it prevents corrosion between ITO and PEDOT. To relieve these problems, several groups introduce evaporated thin metal oxide layer between active layer and top electrode [39,40]. It is thought that comparable V_{oc} and FF with conventional structure could be obtained in inverted structure by modifying energy band structure of intermaterial.

The conceptual mechanism of improved efficiency using nanoporous titania is schematically illustrated in Fig. 5. The excited electrons near the TiO_2 interface could be transport to TiO_2 before being recombined by holes in both flat and nanoporous TiO_2 structures. However, excited electrons far from interface may recombine with holes more frequently prior to transporting to TiO_2 layer than those near the TiO_2 interface. From the same volume of active layer, the excited electrons have shorter traveling distance to TiO_2 in nanoporous structure than in flat one; the more electrons arrive to TiO_2. For such reasons, photovoltaic performance is improved on nanoporous TiO_2 structure.

4. Conclusions

In conclusion, well-ordered nanostructures of TiO_2 were fabricated by the nanoimprinting lithography method with PMMA nanopoles. Moreover, highly crystallized active layer that strongly affect the device performance is observed even with the nanoporous TiO_2 as it is relatively large to crystallize the P3HT inside nanopores. The photovoltaic cells fabricated with ordered nanoporous titania produce more photocurrent; thus PCE was 26% increased than the device with flat titania structure. The reason of improved efficiency results from the efficient charge separation and reduction of effective series resistance by increasing TiO_2–P3HT interface area.

Acknowledgment

This work was supported by Grant no. (ROA-2006-000-10274-0) from the National Research Laboratory Program of the Korea Science & Engineering Foundation.

Appendix A. Supporting Information

Supplementary data associated with this article can be found in the online version at doi:10.1016/j.solmat.2009.04.014.

References

[1] H. Hoppe, N.S. Sariciftci, Morphology of polymer/fullerene bulk heterojunction solar cells, J. Mater. Chem. 16 (2006) 45–61.
[2] B.C. Thompson, J.M.J. Fréchet, Polymer–fullerene composite solar cells, Angew. Chem. Int. Ed. 47 (2008) 58–77.
[3] E. Bundgaard, F.C. Krebs, Low band gap polymers for organic photovoltaics, Sol. Energy Mater. Sol. Cells 91 (2007) 954–985.
[4] S. Günes, H. Neugebauer, N.S. Sariciftci, Conjugated polymer-based organic solar cells, Chem. Rev. 107 (2007) 1324–1338.
[5] F.C. Krebs, J. Alstrup, H. Spanggaard, K. Larsen, E. Kold, Production of large-area polymer solar cells by industrial silk screen printing, lifetime considerations and lamination with polyethyleneterephthalate, Sol. Energy Mater. Sol. Cells 83 (2004) 293–300.
[6] F.C. Krebs, H. Spanggard, T. Kjær, M. Biancardo, J. Alstrup, Large area plastic solar cell modules, Mater. Sci. Eng. B 138 (2007) 106–111.
[7] C. Lungenschmied, G. Dennler, H. Neugebauer, S.N. Sariciftci, M. Glatthaar, T. Meyer, A. Meyer, Flexible, long-lived, large-area, organic solar cells, Sol. Energy Mater. Sol. Cells 91 (2007) 379–384.
[8] W. Ma, C. Yang, X. Gong, K. Lee, A.J. Heeger, Thermally stable, efficient polymer solar cells with nanoscale control of interpenetrating network morphology, Adv. Funct. Mater. 15 (2005) 1617–1622.
[9] G. Li, V. Shrotriya, Y. Yao, Y. Yang, Investigation of annealing effects and film thickness dependence of polymer solar cells based on poly(3-hexylthiophene), J. Appl. Phys. 98 (2005) 043704.
[10] M. Lira-Cantu, F.C. Krebs, Hybrid solar cells based on MEH–PPV and thin film semiconductor oxides (TiO_2, Nb_2O_5, ZnO, CeO_2 and CeO_2–TiO_2): performance improvement during long-time irradiation, Sol. Energy Mater. Sol. Cells 90 (2006) 2076–2086.
[11] M. Lira-Cantu, K. Norrman, J.W. Andreasen, F.C. Krebs, Oxygen release and exchange in niobium oxide MEHPPV hybrid solar cells, Chem. Mater. 18 (2006) 5684–5690.
[12] M. Lira-Cantu, K. Norrman, J.W. Andreasen, N. Casan-Pastor, F.C. Krebs, Detrimental effect of inert atmospheres on hybrid solar cells based on semiconductor oxides, J. Electrochem. Soc. 154 (2007) B508–B513.
[13] D.C. Olson, Y. Lee, M.S. White, N. Kopidakis, S.E. Shaheen, D.S. Ginley, J.A. Voigt, J.W.P. Hsu, Effect of polymer processing on the performance of poly(3-hexylthiophene)/ZnO nanorod photovoltaic devices, J. Phys. Chem. C 111 (2007) 16640–16645.
[14] D.C. Olson, S.E. Shaheen, R.T. Collins, D.S. ginley, The effect of atmosphere and ZnO morphology on the performance of hybrid poly(3-hexylthiophene)/ZnO nanofiber photovoltaic devices, J. Phys. Chem. C 111 (2007) 16670–16678.
[15] F.C. Krebs, Air stable polymer photovoltaics based on a process free from vacuum steps and fullerenes, Sol. Energy Mater. Sol. Cells 92 (2008) 715–726.
[16] F.C. Krebs, Y. Thomann, R. Thomann, J.W. Andreasen, A simple nanostructured polymer/ZnO hybrid solar cell—preparation and operation in air, Nanotechnology 19 (2008) 424013.
[17] Y. Sahin, S. Alem, R. de Bettingnies, J.M. Nunzi, Development of air stable polymer solar cells using an inverted gold on top anode structure, Thin Solid Films 476 (2005) 340–343.
[18] M.Y. Song, K.J. Kim, D.Y. Kim, Enhancement of photovoltaic characteristics using a PEDOT interlayer in TiO_2/MEHPPV heterojunction devices, Sol. Energy Mater. Sol. Cells 85 (2005) 31–39.
[19] M. Jørgensen, K. Norrman, F.C. Krebs, Stability/degradation of polymer solar cells, Sol. Energy Mater. Sol. Cells 92 (2008) 686–714.
[20] K. Kawano, R. Pacios, D. Poplavskyy, J. Nelson, D.D.C. Bradley, J.R. Durrant, Degradation of organic solar cells due to air exposure, Sol. Energy Mater. Sol. Cells 90 (2006) 3520–3530.
[21] N. Koch, A. Vollmer, A. Elschner, Influence of water on the work function of conducting poly(3,4-ethylenedioxythiophene)/poly(styrenesulfonate), Appl. Phys. Lett. 90 (2007) 043512.
[22] M.P. de Jong, L.J. van IJzendoorn, M.J.A. de Voigt, Stability of the interface between indium-tin-oxide and poly(3,4-ethylenedioxythiophene)/poly(styrenesulfonate) in polymer light-emitting diodes, Appl. Phys. Lett. 77 (2000) 2255–2257.
[23] F.C. Krebs, J.E. Carlé, N. Cruys-Bagger, M. Andersen, M.R. Lilliedal, M.A. Hammond, S. Hvidt, Lifetimes of organic photovoltaics: photochemistry, atmosphere effects and barrier layers in ITO–MEHPPV: PCBM–aluminium devices, Sol. Energy Mater. Sol. Cells 86 (2005) 499–516.
[24] K. Norrman, F.C. Krebs, Lifetimes of organic photovoltaics: using TOF-SIMS and $^{18}O_2$ isotopic labelling to characterise chemical degradation mechanisms, Sol. Energy Mater. Sol. Cells 90 (2006) 213–227.
[25] K. Norrman, N.B. Larsen, F.C. Krebs, Lifetimes of organic photovoltaics: combining chemical and physical characterisation techniques to study degradation mechanisms, Sol. Energy Mater. Sol. Cells 90 (2006) 2793–2814.
[26] V. Shrotriya, G. Li, Y. Yao, C. Chu, Y. Yang, Transition metal oxides as the buffer layer for polymer photovoltaic cells, Appl. Phys. Lett. 88 (2006) 073508.
[27] S.W. Tong, C.F. Zhang, C.Y. Jiang, G. Liu, Q.D. Ling, E.T. Kang, D.S.H. Chan, C. Zhu, Improvement in the hole collection of polymer solar cells by utilizing gold nanoparticle buffer layer, Chem. Phys. Lett. 453 (2008) 73–76.
[28] G.K. Mor, K. Shankar, M. Paulose, O.K. Varghse, C.A. Grimes, High efficiency double heterojunction polymer photovoltaic cells using highly ordered TiO_2 nanotube arrays, Appl. Phys. Lett. 91 (2007) 152111.
[29] C. Waldauf, M. Morana, P. Denk, P. Schilinsky, K. Coakley, S.A. Choulis, C.J. Brabec, Highly efficient inverted organic photovoltaics using solution based titanium oxide as electron selective contact, Appl. Phys. Lett. 89 (2006) 233517.
[30] M.S. White, D.C. Olson, S.E. Shaheen, N. Kopidakis, D.S. Ginley, Inverted bulk-heterojunction organic photovoltaic device using a solution-derived ZnO underlayer, Appl. Phys. Lett. 89 (2006) 143517.
[31] H. Liao, L. Chen, Z. Xu, G. Li, Y. Yang, Highly efficient inverted polymer solar cell by low temperature annealing of Cs_2CO_3 interlayer, Appl. Phys. Lett. 92 (2008) 173303.
[32] H.-J. Her, J.-M. Kim, C.J. Kang, Y.-S. Kim, Fabrication of thin film titania with nanopores, nanopoles, and nanopipes by nanoporous alumina template, J. Nanosci. Nanotechnol. 8 (2008) 4808–4812.
[33] K.M. Coakley, M.D. McGehee, Conjugated polymer photovoltaic cells, Chem. Mater. 16 (2004) 4533–4542.
[34] K.M. Coakley, Y.X. Liu, M.D. McGehee, K.L. Frindell, G.D. Stucky, Infiltrating semiconducting polymers into self-assembled mesoporous titania films for photovoltaic applications, Adv. Funct. Mater. 13 (2003) 301–306.
[35] T. Kawahara, Y. Konishi, H. Tada, N. Tohge, J. Nishii, S. Ito, A patterned TiO_2(Anatase)/ TiO_2(Rutile) bilayer-type photocatalyst: effect of the Anatase/Rutile junction on the photocatalytic activity, Angew. Chem. 114 (2002) 2935–2937.
[36] K.C. Lim, C.R. Fincher Jr., A.J. Heeger, Rod-to-coil transition of conjugated polymer in solution, Phys. Rev. Lett. 50 (1983) 1934–1937.
[37] O. Inganas, W.R. Salaneck, J.E. Osterholm, J. Laakso, Thermochromic and solvatochromic effects in poly(3-hexylthiophene), Synth. Met. 22 (1988) 395–406.
[38] S.K. Hau, H. Yip, O. Acton, N.S. Baek, H. Ma, A.K.Y. Jen, Interfacial modification to improve inverted polymer solar cells, J. Mater. Chem. 18 (2008) 5113–5119.
[39] C. Tao, S. Ruan, X. Zhang, G. Xie, L. Shen, X. Kong, W. Dong, C. Liu, W. Chen, Performance improvement of inverted polymer solar cells with different top electrodes by introducing a MoO_3 buffer layer, Appl. Phys. Lett. 93 (2008) 193307.
[40] G. Li, C.W. Chu, V. Shrotriya, J. Huang, Y. Yang, Efficient inverted polymer solar cells, Appl. Phys. Lett. 88 (2006) 253503.